The 2009 IEEE/RSJ International Conference on
Intelligent Robots and Systems
October 11-15, 2009 St. Louis, USA

A Body Sensor Network for Tracking and Monitoring of Functional Arm Motion

Kim Doang Nguyen, *Student Member ,IEEE*, I-Ming Chen, *Senior Member, IEEE*, Zhiqiang Luo, *Member, IEEE,* Song Huat Yeo, Henry Been-Lirn Duh, *Senior Member IEEE*

***Abstract*— In this paper, we present a novel sensing technique, Optical Linear Encoder (OLE), in which the motion of an optical encoder on a reflective strip is converted to limb joints' goniometric data. A body sensing module is designed to integrate the OLE and an accelerometer. A sensor network of three sensing modules is established via Controller Areas Network (CAN) bus to capture full motion of human arm with a 7-DOF kinematic model, proving that OLE can compensate the singularity of the accelerometer which lacks of heading measurement. In addition, a statistical study was conducted to confirm the repeatability and reliability of our sensor network. Results demonstrate that the sensor system has strong potential to be used as a low-cost tool for motion capture, and objective arm function evaluation for both short-term and long-term monitoring.**

***Index Terms*— Wearable sensors, human motion capture and analysis, sensor network**

I. Introduction

THE uses of motion capture technologies have revolutionized variety of disciplines, ranging from medicine, entertainment to art. Huge free databases, such as [1] and [2], as well as other commercial repositories have been proliferating in the response to the growing demand for human motion data. However in the most of current motion tracking systems, inflexibly confine working spaces are requisite. This hinders the widespread latitude of using motion capture in low-end applications. In addition according to the review by Welch et al [3], all current capture systems are very far from the ideal tracker-on-a-chip. Moreover there are very limited sensing technologies, while algorithms that edit, transform, interpolate, and recompose motion data are abundant.

Motion tracking technologies can be classified into five categories, including mechanical, optical, acoustic, inertial/magnetic and fiber-optic tracking systems. Most are dependent on an artificially generated source and are thus range-limited and susceptible to interference and noise. Mechanical capture systems use an exoskeleton that is attached to the articulated structure to be tracked. Rigid or flexible goniometers are utilized to directly measure the joint angle of user's body, for example *Gypsy6* of *Animazoo* [4]. Optical tracking systems track motion of objects by using several cameras to track predefined points on mobile objects within a constrained volume [5], such as *Qualisys* [6] and *Vicon* [7]. In Inertial/Magnetic tracking systems, such as *IGS-190* [8] and *Moven* [9], attachment of Inertial/Magnetic Units (IMU) to each of the major limb segments of a human allows us to independently determine the orientation of each segment [10]. In ultrasonic tracking systems, users carry an ultrasonic microphone or tracker that is connected to a radio transmitter. The microphone acquires ultrasonic pulses sent from four speakers located along the edges of the performance space and radios them back to a computer. Based on the time between each pulse being sent and its arrival at the microphone, the microphone's 3D position is found [11]. Fiber-optic systems, like *ShapeWrap* of *Measurand*, compare light between two ends of an optical fiber to estimate angles [12], [13]. *ShapeWrap* is composed of four bend-twist sensor strips and three IMUs. The four strips are positioned along the two arm and the two legs to measure the motion of the limb segment.

In this project, we explore the design of a motion tracking system, which is capable of recording and reconstructing human arm movement without a restrictive working space. Our design is small and compact enough to be embedded into clothes while retaining comfort. The system captures linear and orientation information from sensing modules worn on the human body. Linear information, which is given by Optical Linear Encoder (OLE) wrapping around joints, is utilized to estimate joint angles. MEMS-based accelerometer provides acceleration and orientation of the limb segment on which the sensing module is attached. The fusion of an accelerometer with the new OLE provides a complete system that is able to track the limb segment's orientations, accelerations and joint angles. By using a sensor network connected by CAN bus, the OLEs can remedy the accelerometer's lack of heading and rotation about the gravitational axis measurement.

Our system is the first tracking system which uses OLEs and the combination of OLEs and accelerometers to motion capture. The simplicity in technology allows us to minimize the production cost (cost of OLE + accelerometer + micro-controller is approximately (USA) \$10+\$15+\$5 = \$30, respectively). Although the best reconstructed human motion data are still not perfect, but the data's quality, along with the sensing module's compact size and improved versatility, wearability, suggest that our system may find wide range of applications in rehabilitation, healthcare, game, virtual reality, human-robot interaction, and so on.

II. SENSING MODULE PROTOTYPE

The wearable sensing module is self-contained, consisting of an Optical Linear Encoder (OLE), an accelerometer, a Digital Signal Controller (DSC), and a CAN controller. The works presented by [14] and [15] also offered various test to assess the accuracy, repeatability and performance of the OLE against other commercial motion capture system, and error analysis of the accelerometer respectively.

A. Optical Linear Encoder (OLE)

1) Working principle

In order to obtain angle of human joint (e.g. elbow), sensing module is attached on one human limb segment (e.g. upper arm), while the module's encoder is connected to a fixed point on the other limb segment (e.g. lower arm) by a wire. The linear encoder slides freely along its longitudinal axis which is collinear with the wire's axis. As the elbow (joint radius R) bends, for instance, the elbow skin is stretched, increasing the length from the sensor to the fixed point. The wire pulls the encoder to move relatively upon the reflective strip with a distance exactly equal to that length difference, Δx, as shown in Fig. 1. The linear displacement, Δx, is captured by the encoder. So the joint angles is estimated using equation (1):

$$\alpha = \frac{\Delta x}{R} \cdot \frac{360^\circ}{2\pi} \tag{1}$$

A scale factor (SF) is inserted into the equation (1) to compensate biometric effects, which may disturb the tracking:

$$\alpha = SF(\alpha_c) \cdot \frac{\Delta x}{R} \cdot \frac{360^\circ}{2\pi} \tag{2}$$

$SF(\alpha_c)$ is a function of calibrating joint angle α_c:

$$SF(\alpha_c) = 2\pi \cdot \frac{\alpha_c}{360^\circ} \cdot \frac{R}{\Delta x_c} \tag{3}$$

The scale factor is obtained through a calibrating process:

- Joint poses predefined gestures (0°, 30°, 60°, 90°, etc)
- Δx_c is recorded from the OLE reading
- $SF(\alpha_c)$ is computed by equation (3)
  - A look-up table is formed and $SF(\alpha_c)$ with respect to each value of α_c is interpolated from the table

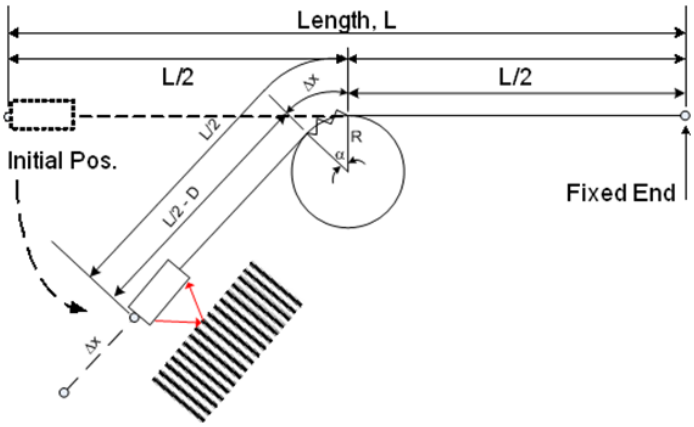

Fig. 1. OLE working principle - conversion of displacement to angle.

2) Mechanical design

A miniature linear encoder is made to slide over a Delrin base structure as shown in Fig. 2. The encoder is attached to a flexible stainless steel wire that has a diameter of 1mm. It is guided by a Teflon tube to restrict it to one DOF. The linear code strip is adhered to the base structure. The base structure's function is to allow the encoder to traverse above the linear code strip while maintaining a constant gap of about 0.4 mm between the code strip and linear encoder.

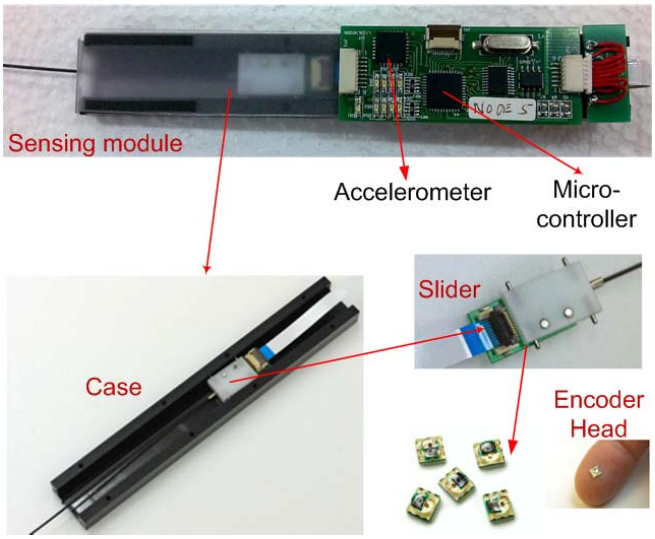

Fig. 2. Components of the sensing module prototype

B. Accelerometer

In static condition of accelerometers, the gravity vector is composed by the three orthogonal accelerations. Hence:

$$\theta = \sin^{-1}\left(\frac{a_x}{g}\right), \text{ and } \phi = \sin^{-1}\left(\frac{a_y}{g \cdot \cos\theta}\right) \tag{4}$$

$[a_x\ a_y\ a_z]^T$ is gravity vector measured in its local coordinate; θ and φ are pitch and roll angles in the global coordinate. Yaw angle cannot be estimated by the accelerometer.

III. SENSOR NETWORK COMMUNICATION

To capture the motion of human arm, three sensing modules and a Data Concentrator are connected to form a sensor network, in which all communications among the sensor nodes and data concentrator are performed by CAN bus as illustrated in Fig. 3. The modules are connected to the bus in a daisy-chain fashion. All nodes in the network have the common component structure. The Microchip's dsPIC33F32MC204 microprocessor executes the firmware, which constantly polls analog signal from the accelerometer LIS3LV02DQ and digital signal from the OLE, and then queue the combined data via SPI port to the Microchip's MCP2515 CAN controller, which handles transmitting, receiving and filtering of message packets, and allows its host module to communicate with other nodes on the sensor network via the CAN bus. The signals are converted to the CAN bus voltages ranging from 0 to 5 volts, with a shift of ±12V by the CAN driver chip MCP2551.

Data Concentrator acts as a gateway to control the behaviors of the sensor nodes, and communicate with other application devices. In our sensor network, CAN bus plays as a broadcast type of bus, in which all nodes can "hear" all transmissions. There is no way to send a message to just a specific node; all nodes will invariably pick up all traffic. Yet using a message filter, embedded in nodes' firmware, each node responds only on a specific message.

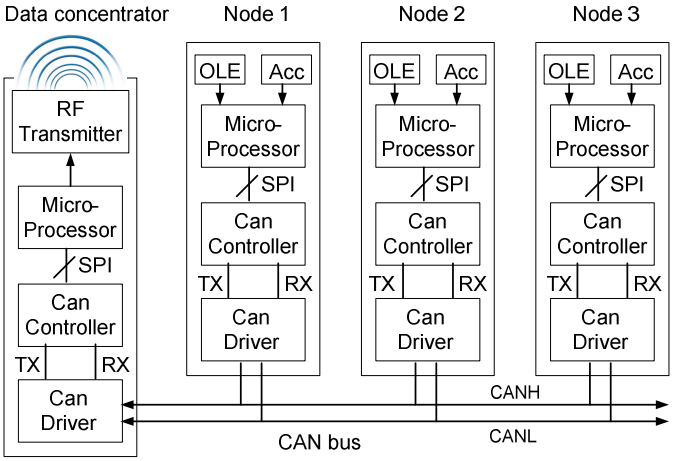

Fig. 3. Motion capture sensor network block diagram

Data acquisition start as the PC sends to the data concentrator a request with the following structure:

<type> <location> <nodeID>

The request specifies data type, node location and ID. Data Concentrator in turn collects the respective information from the interested nodes via the CAN bus, and then sends back to the PC, by a wireless transmitter, with the message structure:

<type> <location> <nodeID> <encoder> <X> <Y> <Z>

The reply includes the configuration information, and the respective encoder readings, as well as acceleration along x-, y-, and z- axes of the accelerometer.

An RF station is designed plugged into the computer via USB port to get the motion data from the sensor network. The RF station runs with TinyOS operating system designed for wireless embedded sensor networks. If the station is detected, the Data Concentrator will establish the communication using ZigBee protocol. Handshaking between the Data Concentrator and the RF station is controlled by the Media Access Control layer as specified by the IEEE 802.15.4 standard.

IV. Sensor Placement and Arm Kinematic Model

A. Placement of OLEs on human arm

As explained, OLE can be used to measure the joint angle in a very simple and clear way, converting linear displacement recorded by the encoder into the joint angle. An extensive study on biomechanics and structure of human arm was conducted to determine the placement of OLEs on joints to record arm motions most effectively [15].

1) Shoulder joint

The shoulder complex has three joints: acromioclavicular, sternoclavicular and glenohumeral, which is a ball and socket joint that allows the arm to rotate in a circular fashion and to hinge out and up away from the body and around it. Hence the sensor is fixed on the upper arm while the fixed end is placed at the top of acromial arch as shown in Fig. 4 (left). When the arm moves horizontally around the body, the sensor will move relatively to the fixed end, and, therefore, gives the data indicating the rotation (the other two rotations are tracked by the accelerometer of the same sensor node).

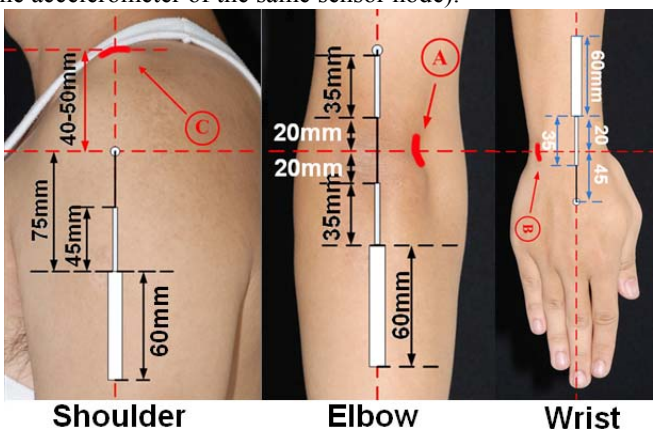

Fig. 4 Placement of the OLEs on shoulder, elbow and wrist joints

2) Elbow joint

The elbow joint is a ginglymus or one-DOF hinge joint, formed by three bones: the humerus of the upper arm, and the paired radius and ulna of the forearm. Placement of the sensor for the elbow is rather simple: the fixed cable end-point is placed as reference point on the upper arm while OLE will be placed on the forearm, as depicted in Fig. 4 (middle). The pulling wire is ensured to pass through the olecranon so that the OLE responds most sensitively to the elbow rotation.

3) Wrist joint

The wrist, a condyloid articulation allowing 3-DOF, is formed by double row of small short bones, carpals, twisted to form a malleable hinge. To capture the wrist flexion and hyperextension motion (other rotations are given by the accelerometer), the OLE is attached on the back of forearm, and the fixed cable end-point is on the back of hand, see Fig. 4 (right). The encoder will travel toward the elbow when in hyperextension and toward the wrist when in flexion.

B. Kinemetic model of human arm

Fig. 5 illustrates the coordinate frames established by D-H procedure. The transformation matrix from frame *(i-1)* to *i* is formulated based on the coordinate arrangement in Fig. 5:

$$T_i^{i-1} = \begin{bmatrix} c\theta_i & -c\alpha_i s\theta_i & s\alpha_i s\theta_i & a_i c\theta_i \\ s\theta_i & c\alpha_i c\theta_i & -s\alpha_i c\theta_i & a_i s\theta_i \\ 0 & s\alpha_i & c\alpha_i & d_i \\ 0 & 0 & 0 & 1 \end{bmatrix} \quad (5)$$

Here θ_i is the joint angle from the x_{i-1} axis to the xi axis measured about z_{i-1} axis; d_i is the distance between frames i-1 and i; a_i is the distance from the intersection of z_{i-1} axis and x_i axis to the i^{th} frame; and α_i is the offset angle from z_{i-1} axis to z_i axis measured about x_i axis. The specific values of these D-H parameters are listed in Table I.

TABLE I
D-H PARAMETERS

Joint i	θ	α	d	a
0	θ_1	90	0	0
1	θ_2	-90	0	0
2	θ_3	90	0	0
3	θ_4	0	d_3	a_3
4	θ_5	90	d_4	a_4
5	θ_6	-90	0	0
6	θ_7	-90	0	0

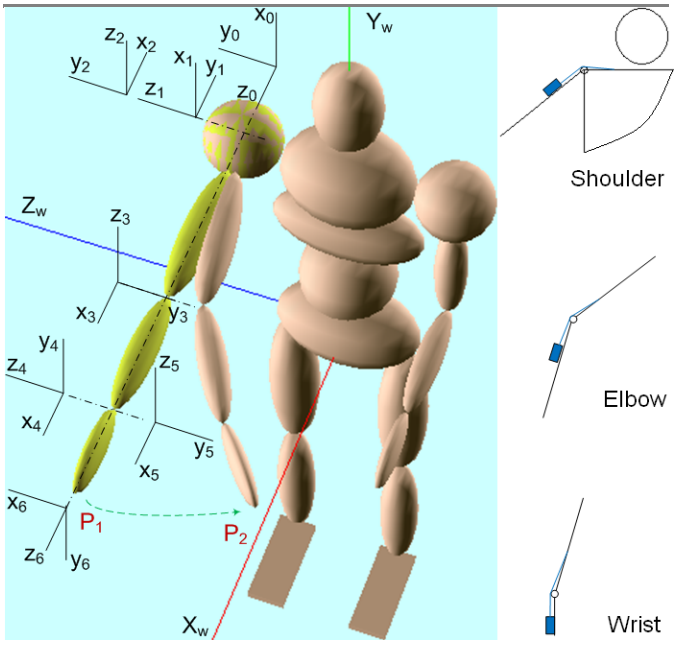

Fig. 5. Denavit-Hartenberg coordinate system for human arm

It is noted that: θ_{ij} is the variable angle of the transformation matrixes from frame i to frame j, T_j^i; θ_k is the variable angle of the transformation matrixes from frame (k-1) to frame k; and the subscript w stands for the world coordinate system.

At shoulder complex, the absolute angles θ_{w0} and θ_{w1} are given by the accelerometer on the upper arm (of the 1st sensing unit, node 1). The OLE of the same node measures θ_2.

The relative angle between upper and forearm, provided by the OLE of node 2, indicates elbow joint angle θ_3.

Wrist rotation θ_5, a singularity to the accelerometer, is recorded by the OLE of node 3. The accelerometer attached on the hand tracks the absolute angles θ_{w4} and θ_{w6}.

The joint angle θ_0 is the rotation angle from the world coordinate system to frame 0, so equal to θ_w. Now we have:

$$T_1^w = T_0^w . T_1^0 \tag{6}$$

Hence,
$$T_1^0 = \left[T_0^w\right]^{-1} . T_1^w \tag{7}$$

Since T_0^w and T_1^w are known as θ_{w0} and θ_{w1} are known, T_1^0 would be determined by (7), and so is θ_1. To find θ_4, which is the variable of the matrix T_4^3.

$$T_4^w = T_0^w . T_1^0 . T_2^1 . T_3^2 . T_4^3 \tag{8}$$

i.e.
$$T_4^3 = \left[T_3^2\right]^{-1} . \left[T_2^1\right]^{-1} . \left[T_1^0\right]^{-1} . \left[T_0^w\right]^{-1} . T_4^w \tag{9}$$

As T_0^w, T_1^0, T_2^1, T_3^2 and T_4^w are known (θ_{w0}, θ_1, θ_2, θ_3 and θ_{w4} are all known), T_4^3 is computed from (9), and so is θ_4. Now the transformation from the world frame to Frame 6 is as follows:

$$T_6^w = T_0^w . T_1^0 . T_2^1 . T_3^2 . T_4^3 . T_5^4 . T_6^5 \tag{10}$$

$$\rightarrow T_6^5 = \left[T_5^4\right]^{-1} . \left[T_4^3\right]^{-1} . \left[T_3^2\right]^{-1} . \left[T_2^1\right]^{-1} . \left[T_1^0\right]^{-1} . \left[T_0^w\right]^{-1} . T_6^w \tag{11}$$

Because θ_{w0}, θ_1, θ_2, θ_3, θ_4, θ_5 and θ_{w6} are all either given by the sensors or calculated previously, so T_0^w, T_1^0, T_2^1, T_3^2, T_4^3 and T_5^4 are known. Therefore T_6^5 is calculable from (11). Thus θ_6 can be computed from the matrix T_6^5.

V. EXPERIMENTAL RESULTS OF STATISTICAL TESTS

The repeatability and reliability of the sensor unit were tested when the user wore the sensor network on the human body. Specifically, one arm suit was designed to include shoulder, elbow and wrist modules to the proper positions discussed in Section IV, as seen in Fig. 6. Each suit module wrapped up one sensor unit to detect the joint movement.

A. Experimental procedures

1) Subjects

Five healthy individuals, male, aged 25-30 years, with no movement disorders in the arm and hand participated in the repeatability and reliability studies.

2) Repeatability testing and reliability analysis

Repeatability was performed by using one arm-reaching task. To perform this task, subjects wearing the arm suit drove the virtual arm to reach a virtual ball above the virtual arm in the simulation environment. The virtual ball was controlled to move along one predefined route. The subjects were required to move the arm to drive the virtual arm to follow the virtual ball. In fact the virtual environment simulates a real rehabilitation test. The detailed procedure, as shown in Fig., 6 is that the arm (a) first lifts up and when the shoulder pitches to the maximal angle, (b) the elbow starts bending to the maximal angle and then returns; when the forearm and upper arm lie in one line, (c) the wrist starts bending to the maximal angle and then returns; (d) the wrist starts rolling to touch ball and then back; after that, the whole arm returns to the initial position. All three joints, shoulder, elbow, and wrist, needed to rotate from the initial rest state to the maximum tension state and then return. Each subject was required to perform the arm-reaching task for 10 trials.

B. Analysis

1) Repeatability testing

Each raw data file (one subject) contained one data block of 10 trials of reaching the ball. For each of the 10 trials, 4 sensors detected the corresponding joint movement and each sensor collected 1000 sample data during the arm-reaching task. Therefore, the task performed by each subject can be

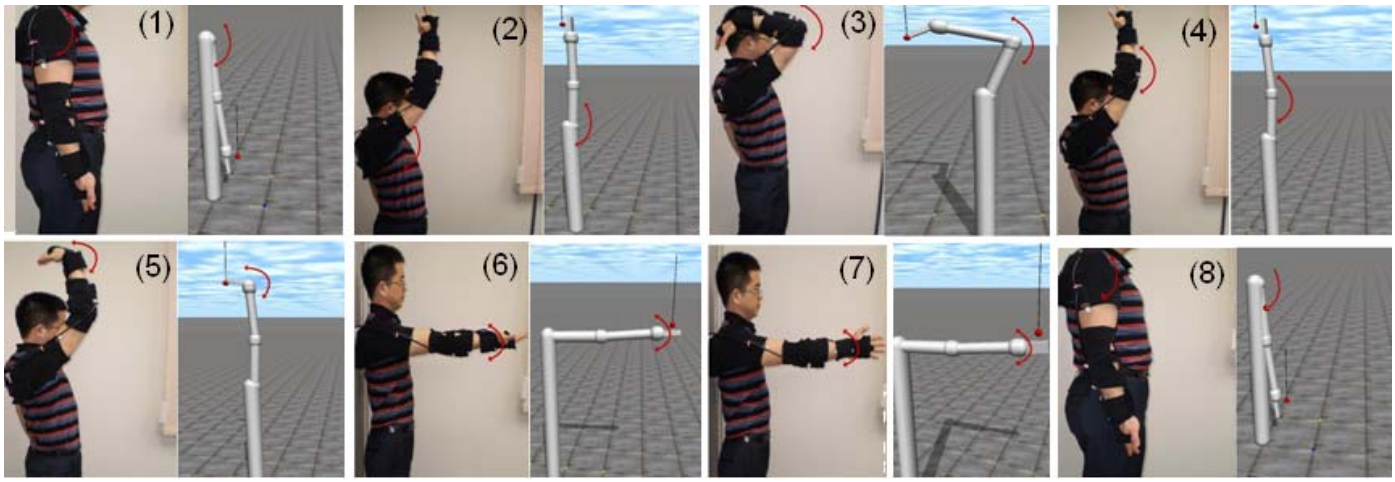

Fig. 6 Arm movement testing procedure: (1) Initial gesture); (2) Lift arm as vertical as possible; (3) bend elbow backwards; (4) return to the gesture in (2); (5) bend wrist backwards, then return to the gesture in (2); (6) move the arm to horizontal gesture; (7) Roll the wrist then move back; (8) return to the gesture in (1)

represented by a three-dimensional array of data $\{X_{ijk}\}$, i = 1,…, 10, j = 1, …,10, k = 1, …,4 to specify the i^{th} position in the j^{th} trial (subject) for the k^{th} sensor. The maximum and minimum trial data averages were used to establish the range of each sensor. Range is computed by the functions in [16]:

$$R_k = \max_j \overline{X}_{jk} - \min_j \overline{X}_{jk} \quad (12)$$

Where

$$\overline{X}_{jk} = \frac{1}{10}\sum_{i=1}^{10} X_{ijk} \quad (13)$$

From individual data block ranges (R_k) and standard deviations (SD) of the X_{jk} values, overall value of average range and average SD across all subjects was computed.

2) *Reliability analysis*

Reliability analysis was conducted by computing an Intra-class coefficient (ICC) to identify the source of variability between measures. ICC values close to 1 indicate high internal consistency in the measurement method, giving confidence that the test results reflect true scores. Reliability analyses were performed by randomly selecting 2 of the 5 data block per each sensor, and further randomly selecting 1 of the 10 trials within each data block, and then ICC was computed for these two trials in. This was repeated 20 times.

C. *Results*

1) *Repeatability*

A single data block file contains 10 trials of performing the arm-reaching task is shown in Fig. 7. It should be noted that the angle of the shoulder joint was coded to range from -90^0 to 90^0. Each data block produced 4 average values for our sensors. Five such data block files were processed to produce 5 average values for each sensor, as shown in Fig. 8.

2) *Reliability*

ICC analysis was performed for each sensor. The average ICC for each sensor ranged from 0.959 to 0.975 with an overall average of 0.967±0.08, as seen in Table II.

D. *Discussion*

The sensor network was attached on the arm and evaluated for repeatability and reliability. We designed a protocol to test the sensor by asking subjects to perform an arm-reaching task. Further, we reduced the degrees of freedom to yield reasonably accurate results with a significantly lower measurement and data processing burden. The average error range is 2.819^0 (average of the ranges in Fig. 9). In addition, the average SD is 0.697^0 (average of the SD in Fig. 9). Reliability analysis showed high ICC values for all channels within 0.959-0.975 with an overall average of 0.967, showing our system's ability to perform and maintain its functions in routine circumstances, with different biometric subjects.

The current implementation of the system was limited to three sensors to measure four out of 7 DOFs of shoulder, elbow and wrist joint movements. This number of DOFs can be expanded to 7 DOFs without big changes to the hardware.

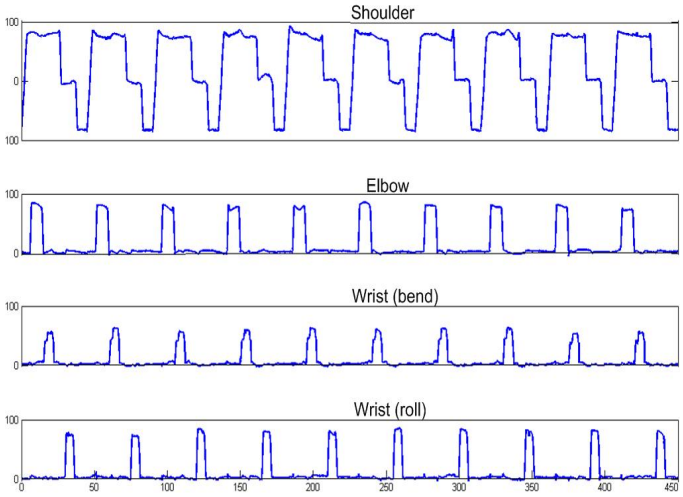

Fig. 7 Raw data from each joint for a single data block collected during the performance of the arm-reaching task. Angles (the vertical dimension) are in degrees. Time (the horizontal dimension) is in seconds. As arm lies horizontally, the degree of the shoulder joint is 0 degree. As upper arm, forearm and hand lie in one line, the angles of both elbow and wrist (bend) are 0 degrees. Wrist roll is the relative angle of hand with respect to forearm.

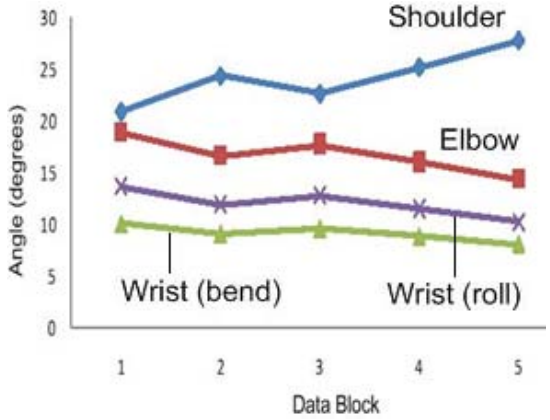

Fig. 8 . Individual data block averages for repeatability. Each value is the average of 10 cycles of the arm-reaching task for each sensor per subject.

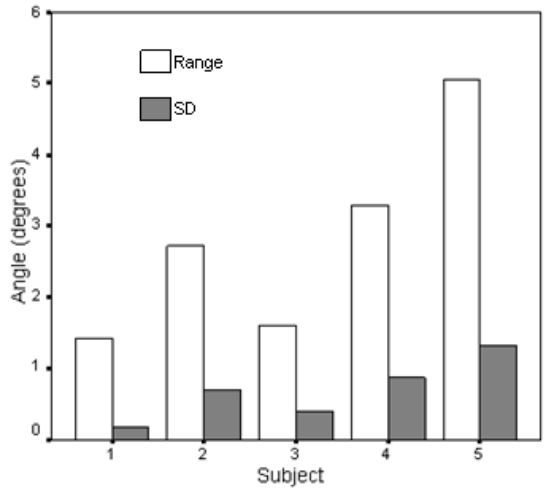

Fig. 9. Average range and standard deviation (SD) for each subject.

TABLE II
INTRA-CLASS CORELATION COEFFICIENT OF RELIABILITY

Shoulder	Elbow	Wrist (bend)	Wrist (roll)	Average
0.975	0.974	0.959	0.962	0.967

VI. CONCLUSION

We have presented the design of the OLE for the function of capturing human motion. The encoder track the distance it travels upon a code-strip. When the sensing module is worn properly on human body, the recorded distance can be converted to joint angles. Various experiments were conducted to test the performance of the OLE for the purpose of tracking motion. In the off-body comparison test, OLE showed the correlation coefficient of 0.999 and RMS error of 1.2 with respect to PowerCube [14]. In the on-body test, compared with Goniometer, OLE performs the correlation coefficient of 0.990 and RMS error of 3.8^{o}; compared with ShapeWrap, OLE perform the correlation coefficient of 0.992 and RMS error of 3.1^{o}. Hence the performance of the OLE is comparable to that of other commercial human motion capture systems. Three sensing nodes were formed into a sensor network through CAN bus for the function of capturing free motion of human arm. A kinematic model of human and a placement protocol of the sensing module were proposed so that information from the OLEs can compensate the lacked information of accelerometers (rotation about vertical axis and heading direction). Experiments were carried out to test repeatability and reliability of the sensor networks. The average error range was 2.819^{0}. In addition, the average standard deviation was 0.697^{0}. Reliability analysis showed high ICC values for all channels within 0.959-0.975 with an overall average of 0.967. These tests prove the ability of our system to perform and maintain its functions in routine circumstances, with different biometric subjects.

There are many possibilities for future works. First, we could extend the system to a full-body motion capture system to record motion of the entire human body. The system could be converted to a gaming device. Moreover, the system would find wide range of applications in the field of healthcare.

ACKNOWLEDGEMENT

The authors would like to thank Kwang Yong Lim, Young Koon Goh and Wei Dong for their contributions to this project. This work was supported in part by the Agency for Science, Technology and Research, Singapore, under SERC Grant 0521180050, and Media Development Authority, Singapore under NRF IDM004-005 Grant.

REFERENCES

[1] CMU Graphics Lab Motion Capture Database 2008 [Online]. Available: http://mocap.cs.cmu.edu/
[2] Databases or Datasets for Computer Vision Applications and Testing 2008 [Online]. Available: http://datasets.visionbib.com
[3] G. Welch, E. Foxlin, "Motion Tracking: No Silver Bullet, but a Respectable Arsenal," *IEEE Com. Graph. App.*, 22 (6), pp. 24-38, 2002.
[4] Gypsy6 2008 [Online]. Available: www.animazoo.com/Gypsy6.aspx
[5] T. G. Bishop, "Self-Tracker: A Smart Optical Sensor on Silicon", PhD thesis, University of North Carolina at Chapel Hill, 1984.
[6] Qualisys 2008 [Online]. Available: www.qualisys.com.
[7] Vicon 2008 [Online]. Available: www.vicon.com.
[8] IGS-90 2008 [Online]. Available : www.animazoo.com/IGS190.aspx.
[9] Moven 2008 [Online]. Available: www.moven.com.
[10] N. Miller, O. C. Jenkins, M. Kallmann, M. J. Andmatric'c, "Motion capture from inertial sensing for untethered humanoid teleoperation", in *Proc. Int'l Conf. of Humanoid Robotics*, 547–565, 2004
[11] D. Vlasic, R. Adelsberger, G. Vannucci, J. Barnwell, M. Gross, W. Matusik, and J. Popovic´, "Practical motion capture in everyday surroundings," ACM Transaction on Graphics, 26(3), 2007.
[12] L. Danisch, K. Englehart, and A. Trivett, "Spatially continuous six-degrees-of-freedom position and orientation sensor," *Sensor Review*, Vol. 19-2, pp. 106-112, 1999.
[13] Measurand 2008 [Online]. Available: http://www.measurand.com.
[14] K. Y. Lim, F. Y. K. Goh, W. Dong, K. D. Nguyen, I.-M. Chen, S. H. Yeo, H. B. L. Duh, C. G. Kim, "A Wearable, Self-Calibrating, Wireless Sensor Network for Body Motion Processing", in *Proc. IEEE Int. Conf. Robot. Autom.*, pp. 1017 – 1022, California, May 2008.
[15] W. Dong, K. Y. Lim, Y. K. Goh, K. D. Nguyen, I.-M. Chen, S. H. Yeo, and H. B. L. Duh, "A Low-cost Motion Tracker and Its Error Analysis", *Proc. IEEE Int. Conf. Robot. Autom.*, pp. 311 – 316, Pasadena, California, United State, May 2008.
[16] Y. K. Goh , "Development of a wearable motion capture system using linear encoder", Technical report, Nanyang Tech. University, 2009.
[17] L. Dipietro, A.M. Sabatini, P. Dario, "Evaluation of an instrumented glove for hand-movement acquisition", *J. Rehab. Res.,* 40-2, pp.172-90.